

# Structure of an antibody–antigen complex: Crystal structure of the HyHEL-10 Fab–lysozyme complex

(x-ray crystallography/complementarity/discontinuous epitope)

EDUARDO A. PADLAN\*, ENID W. SILVERTON\*, STEVEN SHERIFF\*†, GERSON H. COHEN\*,  
SANDRA J. SMITH-GILL‡, AND DAVID R. DAVIES\*

\*Laboratory of Molecular Biology, National Institute of Diabetes, Digestive and Kidney Diseases, and †Laboratory of Genetics, National Cancer Institute, National Institutes of Health, Bethesda, MD 20892

Contributed by David R. Davies, April 24, 1989

**ABSTRACT** The crystal structure of the complex of the anti-lysozyme HyHEL-10 Fab and hen egg white lysozyme has been determined to a nominal resolution of 3.0 Å. The antigenic determinant (epitope) on the lysozyme is discontinuous, consisting of residues from four different regions of the linear sequence. It consists of the exposed residues of an  $\alpha$ -helix together with surrounding amino acids. The epitope crosses the active-site cleft and includes a tryptophan located within this cleft. The combining site of the antibody is mostly flat with a protuberance made up of two tyrosines that penetrate the cleft. All six complementarity-determining regions of the Fab contribute at least one residue to the binding; one residue from the framework is also in contact with the lysozyme. The contacting residues on the antibody contain a disproportionate number of aromatic side chains. The antibody–antigen contact mainly involves hydrogen bonds and van der Waals interactions; there is one ion-pair interaction but it is weak.

The interaction of antibodies with protein antigens has been the subject of several recent crystallographic investigations. These include complexes of hen egg white lysozyme with the Fab fragments of the monoclonal anti-lysozymes D1.3 (1) and HyHEL-5 (2) and a Fab complex with influenza neuraminidase (3). From these data a common pattern of interaction is emerging (4) in which there is a high degree of complementarity between the interacting surfaces of the antibody and antigen; the epitope is made up of several small, discrete segments of the polypeptide chain; and relatively small conformational changes occur in the antigen as a result of binding. Here we report the x-ray analysis of HyHEL-10 Fab–lysozyme, in which the antigenic site differs from the two previous examples. The results complement the previous studies but differ from them in several ways.

HyHEL-10 is an IgG1( $\kappa$ ) antibody specific for hen egg white lysozyme. The affinity of HyHEL-10 for hen egg white lysozyme, as estimated by PEG immunoprecipitation, is  $1.5 \times 10^9 \text{ M}^{-1}$  (M. E. Denton and H. A. Scheraga, personal communication), slightly lower than that of HyHEL-5, thus making HyHEL-10 intermediate in affinity between HyHEL-5 and D1.3.§

HyHEL-10 expresses a member of the  $V_{H36-60}$  variable gene segment family, the  $DQ52$  diversity gene segment, and the  $J_{H3}$  joining gene segment in the heavy (H) chain and a  $V_{\kappa 23}$  gene and  $J_{\kappa 2}$  in the light (L) chain (9). Thus, HyHEL-10 is structurally distinct from HyHEL-5 (which expresses  $V_{HJ558}$  and  $V_{\kappa 4}$ ) and D1.3 (which expresses  $V_{HQ52}$  and  $V_{\kappa 12/13}$ ).

The publication costs of this article were defrayed in part by page charge payment. This article must therefore be hereby marked "advertisement" in accordance with 18 U.S.C. §1734 solely to indicate this fact.

## MATERIALS AND METHODS

Crystals of the complex of HyHEL-10 Fab with hen egg white lysozyme, grown as described (11), exhibit the symmetry of space group  $P2_12_12_1$  with  $a = 57.47$ ,  $b = 118.73$ ,  $c = 137.68$  Å and one Fab–lysozyme complex per asymmetric unit.

Intensity data were collected with the Mark II multiwire detector system at the University of California, San Diego (12). The  $R$  factor relating the intensities of symmetry-related reflections (12) was 0.066. The data set used in the structure analysis had 12,501 reflections beyond 10.0-Å spacings with  $F \geq 3\sigma(F)$ . These constitute about 78% of the theoretically observable reflections between 10.0- and 3.1-Å spacings; an additional 5% of the reflections between 3.1 and 3.0 Å are present in this data set.

The structure was determined by molecular replacement (13) using a predecessor of the program package MERLOT (14). Rotation and translation searches were performed independently (15) for the lysozyme, Fv (module containing  $V_H$  and  $V_L$ , the variable domains of the H and L chains), and  $C_L/C_{H1}$  (constant domain of L chain/first constant domain of H chain) portions of the structure. In the search for the orientation of the lysozyme and the Fv, the highest peaks in the rotation function turned out to be the correct peaks. The correct peak in the rotation search for the  $C_L/C_{H1}$  was only the seventh highest. The translation search gave unambiguous results in all three cases. Details of the molecular replacement analysis will be published elsewhere (S.S., E.A.P., G.H.C., and D.R.D.). The molecular probes that proved useful in the analysis were hen egg white lysozyme from the refinement analysis of Diamond (16) [Protein Data Bank (PDB) File 6LYZ], the Fv of McPC603 (17) (PDB File 1MCP), and the  $C_L/C_{H1}$  of HyHEL-5 (2) (PDB File 2HFL). The orientations and positions of the various parts of the complex were refined with CORELS (18) allowing the  $V_L$ ,  $V_H$ ,  $C_L$  and  $C_{H1}$  domains and lysozyme to move independently. The structure was then subjected to restrained least-squares

Abbreviations: H, heavy; L, light;  $V_L$  and  $V_H$ , variable domains of L and H chains;  $C_L$  and  $C_{H1}$ , constant domain of L chain and first constant domain of H chain; Fv, module containing  $V_L$  and  $V_H$ ; CDR, complementarity-determining region; CDR $n$ -L or CDR $n$ -H,  $n$ th CDR of L or H chain.

†Present address: Squibb Institute for Medical Research, P.O. Box 4000, Princeton, NJ 08543-4000.

§Using PEG immunoprecipitation at pH 7.2, Denton and Scheraga determined association constants of  $1.5 \times 10^9 \text{ M}^{-1}$  and  $2.5 \times 10^9 \text{ M}^{-1}$  for HyHEL-10 and HyHEL-5, respectively. Lavoie *et al.* (5) determined association constants of  $\approx 4 \times 10^9 \text{ M}^{-1}$  and  $\approx 1.4 \times 10^{10} \text{ M}^{-1}$  at pH 8.2 by the method of Friguete *et al.* (6). The association constant for D1.3 Fab, also determined by the method of Friguete *et al.*, has been reported (7) as  $4.5 \times 10^7 \text{ M}^{-1}$  at pH 7.4; more recently, an association constant of  $1.3 \times 10^8 \text{ M}^{-1}$  was determined by fluorescence quenching (8).

refinement using the program PROLSQ (19, 20) and model rebuilding on the basis of OMIT maps (21) using the graphics

program FRODO (22). The final *R* value was 0.24 with deviations from ideality of 0.011 Å for bond lengths and of 0.034

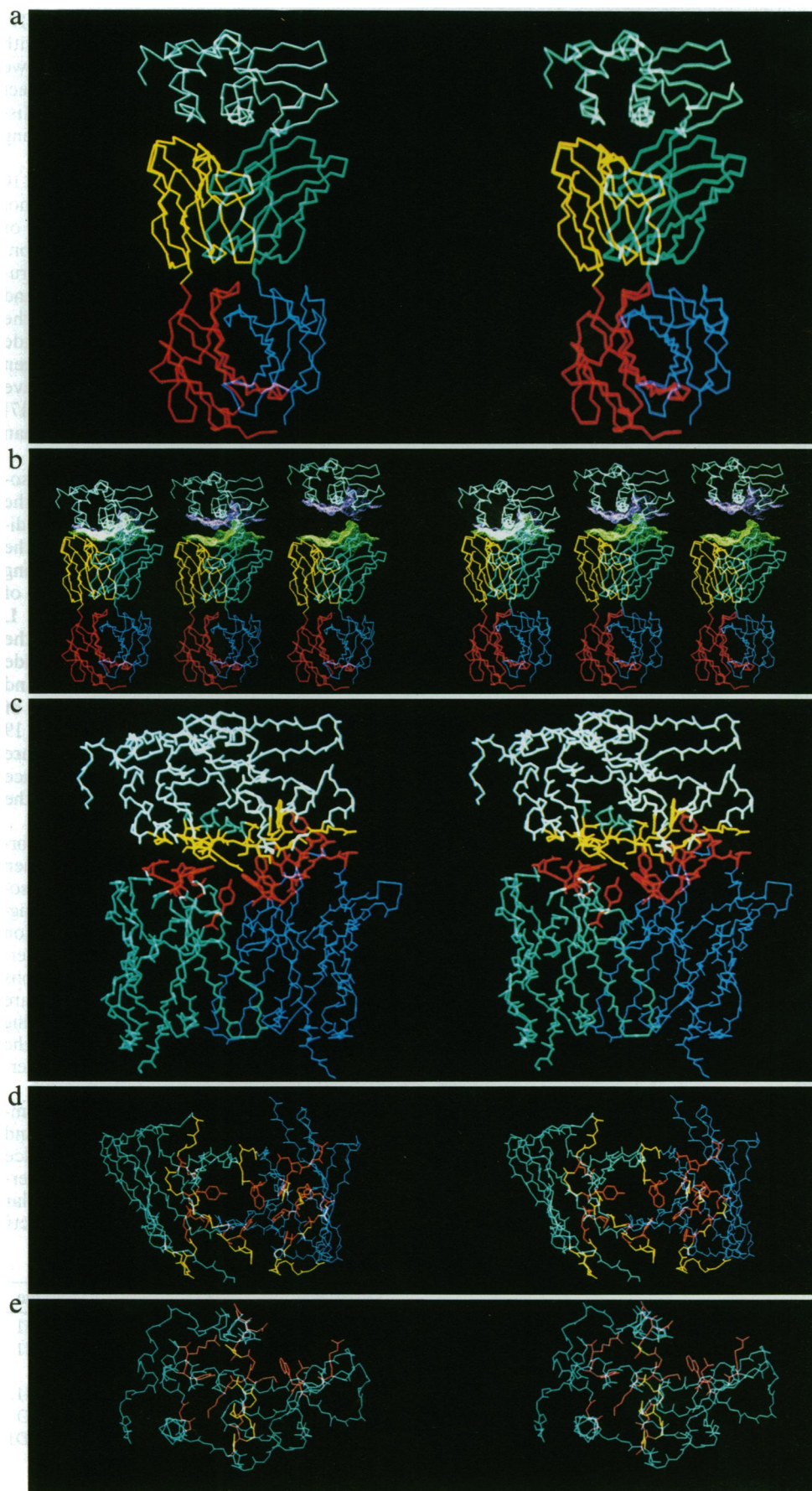


FIG. 1. Stereo diagrams. (a)  $\alpha$ -Carbon trace of the HyHEL-10 Fab-lysozyme complex. Lysozyme is shown in white,  $V_L$  in yellow,  $V_H$  in light blue,  $C_L$  in red, and  $C_H1$  in dark blue. (b) Same as a and showing the interacting surfaces: the surface covering the epitope in green and the surface covering the contacting residues from the Fab in magenta. At left, the complex is as it is in the crystal structure; in the middle and at right, the lysozyme has been separated from the Fab by 7 Å and by 14 Å, respectively. (c) Backbone of HyHEL-10 Fv and lysozyme with the contacting side chains from HyHEL-10 shown in red and those from the lysozyme shown in yellow. The rest of the helical region (lysozyme residues 88-99) and  $V_L$  are shown in light blue, and  $V_H$  is shown in dark blue. (d) HyHEL-10 Fv showing the CDRs in yellow and the contacting residues in red.  $V_L$  is on the left (light blue) and  $V_H$  is on the right (dark blue). (e) The HyHEL-10 epitope on lysozyme showing the contacting residues in red. The helical region 88-99 is shown in yellow and the rest of the lysozyme in light blue.

Å for angle distances and with a deviation from planarity of 0.004 Å. The refined coordinates have been deposited in the Protein Data Bank (23) (File 3HFM). The error in atomic positions was estimated (24) to be 0.4 Å.

Molecular surface representations were computed with the program MS (25) using a probe radius of 1.5 Å and standard van der Waals radii (26). Atomic contacts were defined according to the criteria of Sheriff *et al.* (27). The various domains of HyHEL-10 Fab were compared with the following immunoglobulin structures: McPC603 and J539 (28) (PDB File 1FBJ), HyHEL-5 and D1.3 (courtesy of R. Poljak, Pasteur Institute), KOL (29) (PDB File 1FB4), NEW (30) (PDB File 3FAB), and REI (31) (PDB File 1REI). Least-squares superposition of structures was accomplished with the program ALIGN (written by G.H.C.); only  $\alpha$  carbons were used in the superpositions. ALIGN reports the individual deviations and the rms deviation between structurally equivalent pairs of atoms. The numbering scheme used here for the HyHEL-10 residues follows the convention of Kabat *et al.* (32).

## RESULTS

**Overall Structure.** Fig. 1a shows the  $\alpha$ -carbon trace of the HyHEL-10 Fab-lysozyme complex. The contact between lysozyme and HyHEL-10 involves the complementarity-determining regions (CDRs) of the antibody with the exterior of the lysozyme helix (residues 88-99) and some surrounding amino acid residues. The two interacting surfaces (Fig. 1b) are strikingly complementary so that solvent is completely excluded from the interface. The helix in the epitope is oriented diagonally across the combining site so that its N terminus interacts with the second CDR of the L chain (CDR2-L) whereas its C terminus and the segment beyond it interact mainly with CDR1-H and CDR2-H (Fig. 1c and d; Table 1).

**The Epitope.** The lysozyme epitope for HyHEL-10 is quite discontinuous, consisting of residues coming from distant parts of the linear sequence but made contiguous by the folding of the protein. The area of lysozyme that is in contact with the antibody is 774 Å<sup>2</sup>.

The lysozyme residues that contact the antibody are His-15, Gly-16, Tyr-20, and Arg-21, which are on one side of the helix; Thr-89, Asn-93, Lys-96, Lys-97, and Ile-98, which

constitute the external surface of the helix; Ser-100, Asp-101, and Gly-102, which extend beyond the helix; Trp-63, which is in the active-site cleft; and Arg-73 and Leu-75, which are on the other side of the cleft (Fig. 1e). In addition, Asn-19, Asn-103, and Ala-107 are partly buried by the interaction with the antibody, although not in actual contact by the criteria we have used. Four of these residues participate in the contact with the antibody only through their main-chain atoms (His-15, Gly-16, Ile-98, and Gly-102). Most of the contacting residues are polar and five of them are charged.

**Structure of the Combining Site.** The surface of HyHEL-10 that interacts with lysozyme is unusual in that it is not noticeably concave and contains no pronounced grooves or cavities. On the contrary, the surface has a large protrusion, which fits into the active-site cleft of lysozyme. This protrusion is formed by the side chains of Tyr-33 from CDR1-H and Tyr-53 from CDR2-H (Fig. 1b). The interacting surface of the antibody contains a disproportionate number of aromatic side chains that point outward and that interact with the antigen (Fig. 1c; Table 1). Large numbers of aromatic residues have also been observed in the combining sites of McPC603 (17) and D1.3 (1) and in the presumed binding site of the human class I major histocompatibility antigen A2 (33).

All six CDRs participate in the interaction with the lysozyme. The CDRs of the L chain contribute 8 residues to the contact and those of the H chain contribute 10. One additional residue from the H chain, Thr-30, comes from the framework. CDR2-H has the largest number of contacting residues with 6, while CDR3-H has only 1 (Table 1). For 3 of the residues (Gly-30, Ser-91, and Asn-92, all from the L chain), only their main-chain atoms are involved in the contact. Seven of the contacting residues have aromatic side chains: Tyr-50 and -96 from the L chain; Tyr-33, -50, -53 and -58 and Trp-95 from the H chain. Only one side chain, that of Asp-32 of the H chain, is charged. In addition to the 19 contacting residues, Ser-93 and Trp-94 of the L chain are partly buried by the interaction with the antigen. The surface area on the antibody that is buried by the interaction with the lysozyme is 720 Å<sup>2</sup>.

**Conformational Changes in the Antigen.** No major conformational changes occur in the structure of the lysozyme when it binds to HyHEL-10. Comparison of the complexed lysozyme with the uncomplexed structure (coordinates of tetragonal lysozyme courtesy of D. C. Phillips) gives a rms deviation of 0.47 Å for corresponding  $\alpha$  carbons, with significant differences occurring at positions 47, 101, and 102 having deviations of 1.44, 1.80, and 2.13 Å, respectively. Larger differences are found for the side chains, most notably with the aromatic ring of Trp-62, which has been rotated by 150 degrees about the C <sup>$\beta$</sup> -C <sup>$\gamma$</sup>  bond presumably in order to avoid close steric interactions with a tyrosine side chain from the antibody.

**Forces Between the Antibody and the Antigen.** The complementarity of the contacting surfaces of HyHEL-10 and lysozyme is so great that there are no cavities in the interface large enough to accommodate a water molecule. The interaction between the two proteins (Fig. 1c) consists of polar and apolar interactions; of the 126 pairwise atomic contacts

Table 1. HyHEL-10 residues in contact with lysozyme

HyHEL-10 residue*	Lysozyme residue(s)
<b>V<sub>L</sub></b>	
Gly-30	Gly-16
Asn-31 (h)	His-15, Gly-16, Lys-96
Asn-32 (h)	Gly-16, Tyr-20
Tyr-50	Asn-93, Lys-96
Gln-53 (h)	Thr-89, Asn-93
Ser-91 (m)	Tyr-20
Asn-92 (m,h)	Tyr-20, Arg-21
Tyr-96 (h)	Arg-21
<b>V<sub>H</sub></b>	
Thr-30†	Arg-73
Ser-31 (h)	Arg-73, Leu-75
Asp-32 (s)	Lys-97
Tyr-33 (h)	Trp-63, Lys-97, Ile-98, Ser-100, Asp-101
Tyr-50 (h)	Arg-21, Ser-100
Ser-52 (h)	Asp-101
Tyr-53 (h)	Trp-63, Leu-75, Asp-101
Ser-54	Asp-101
Ser-56	Asp-101, Gly-102
Tyr-58 (h)	Arg-21, Ser-100, Gly-102
Trp-95	Arg-21, Lys-97, Ser-100

\*Nature of interaction is indicated in parentheses: m, main-chain atoms only; h, hydrogen bonding; s, salt bridge.

†Framework residue.

Table 2. Hydrogen bonds between HyHEL-10 and lysozyme

V <sub>L</sub>	Lysozyme	V <sub>H</sub>	Lysozyme
Asn-31 OD1	Lys-96 NZ	Thr-30 O	Arg-73 NH1
Asn-32 ND2	Gly-16 O	Ser-31 OG	Arg-73 NH1
Gln-53 OE1	Asn-93 ND2	Tyr-33 OH	Lys-97 O
Gln-53 NE2	Asn-93 OD1	Tyr-50 OH	Arg-21 NH1, Ser-100 O
Ser-91 O	Tyr-20 OH	Tyr-53 O	Asp-101 OD1
Asn-92 O	Arg-21 N	Tyr-58 OH	Gly-102 N
Tyr-96 OH	Arg-21 NH1		



(Table 1), 111 are van der Waals contacts and 14 are hydrogen-bonding contacts (Table 2).

Although 6 of the contacting residues—Asp-32 from the H chain and Arg-21 and -73, Lys-96 and -97, and Asp-101 from the lysozyme—are probably charged under the conditions of our experiment, we find only one salt bridge, between Asp-32 from HyHEL-10 and Lys-97 from lysozyme, with a separation of 3.6 Å between the side-chain nitrogen of the lysine and the nearer oxygen in the carboxyl group of the aspartate side chain. This salt bridge is exposed to the solvent and could be weakened by interaction with water molecules.

Some of the hydrogen bonds are between side-chain and main-chain atoms, including several involving the hydroxyl group of tyrosine (Tyr-33, -50, and -58 from the H chain of HyHEL-10 and Tyr-20 of the lysozyme). There is one probable main-chain/main-chain hydrogen bond, involving the carbonyl oxygen of Thr-30 of the H chain and the amide nitrogen of Gly-102 of the lysozyme (Table 2).

The side chain of Tyr-53 from CDR2-H of HyHEL-10 penetrates into the catalytic cleft of the antigen and interacts with Trp-63, which has been implicated in the enzymatic activity of lysozyme (34).

**Structures of the Individual Domains and Conformational Changes in the Antibody.** The structure of the uncomplexed Fab is not yet available. Nevertheless, we believe that no gross conformational changes in the structure of the combining site could have occurred because of the overall similarity of the HyHEL-10 domain structures to those of other Fabs and the similar ways in which they associate.

The Fv ( $V_L/V_H$ ) and  $C_L/C_{H1}$  modules of the Fab have the canonical structures observed in other Fabs. The  $V_H$  of HyHEL-10 is related to the  $V_L$  by a pseudodyad axis (a rotation of 170.7 degrees and a translation of  $-0.3$  Å along this axis). These values fall within the range of values for other Fvs of known structure: 165.9 to 172.6 degrees of rotation and  $-0.9$  to  $0.8$  Å of translation. The pseudodyad axis relating the  $C_{H1}$  to the  $C_L$  of HyHEL-10 yields values of 166.6 degrees of rotation and  $-1.6$  Å of translation along this axis. Again, these values are comparable to those for other  $C_L/C_{H1}$  modules: 167.4 to 173.8 degrees of rotation and  $-3.1$  to  $3.0$  Å of translation. The angle between these two pseudodyad axes—i.e., the elbow bend of HyHEL-10 Fab—is 147 degrees.

Comparison of the framework structure of HyHEL-10  $V_L$  with those of other immunoglobulins reveals that HyHEL-10 is most similar to McPC603 (rms deviation of 0.49 Å), with which it has 53 sequence identities in the 80 framework residues, and to the human myeloma protein REI (rms deviation of 0.55 Å), with which it has 46 identical residues in homologous positions. The  $V_L$  domains of HyHEL-5 and D1.3 also have 53 sequence identities with HyHEL-10 in the framework, but the structural differences are slightly greater for these two domains (rms deviations of 0.71 and 1.02 Å, respectively) than for those of McPC603 and REI. The L-chain CDRs of REI and D1.3 have the same number of residues as those of HyHEL-10, and the superposition of these CDRs gives rms deviations of 0.54 and 1.04 Å, respectively. The sequence similarities of REI and D1.3 to HyHEL-10 in their L-chain CDRs are 13 and 11 residues, respectively, in common out of a total of 27.

Comparison of the framework structure of HyHEL-10  $V_H$  with those of other Fabs reveals that HyHEL-10 is most similar to HyHEL-5, McPC603, and NEW, with rms deviations of 0.83, 0.84, and 0.86 Å and sequence identities of 39, 43, and 54 among the 87 residues in the framework, respectively. HyHEL-10 does not have all three H-chain CDRs with the same lengths as any of the other  $V_H$  domains of known structure. However, CDR1-H and CDR2-H of HyHEL-10 have the same number of residues as the corresponding CDRs of NEW and D1.3. Superposition of these CDRs gives rms deviations of 1.51 and 1.36 Å, respectively; the sequence

similarities are 6 and 7 identical residues out of 21 corresponding CDR positions for NEW and D1.3, respectively. HyHEL-10  $V_H$  has a tyrosine at position 47 instead of the more usual tryptophan (32). The structure of the region around position 47 in HyHEL-10 is essentially unaltered compared to that found in the other  $V_H$  domains of known structure, which all have tryptophan at this position.

The  $C_L$  of HyHEL-10 has the same sequence as those of HyHEL-5, McPC603, and J539. Superposition of these domains gives rms deviations of 0.60, 0.66 and 0.79 Å, respectively. The  $C_L$  of D1.3 has 4 amino acid differences relative to HyHEL-10; superposition of these domains gives a rms deviation of 1.35 Å. The  $C_{H1}$  domains of HyHEL-10 and HyHEL-5 have identical sequences and superposition of these domains gives a rms deviation of 0.78 Å. The  $C_{H1}$  of D1.3 differs from the sequence of HyHEL-10 at 2 positions and the corresponding  $\alpha$  carbons differ with a rms deviation of 1.25 Å.

The CDRs of HyHEL-10 are short. CDR1-L with 11 residues and CDR3-L with 9 are both only one residue longer than the shortest of these regions known so far (32). CDR2-L with 7 residues and CDR1-H with 5 have the usual number of amino acids in these regions. CDR2-H with 16 residues (longest known has 19; ref. 32) and CDR3-H with 5 (longest known has 19) represent the shortest of these regions in the structures of Fabs. The CDR residues of HyHEL-10 provide a total hypervariable surface area of 2220 Å<sup>2</sup>.

## DISCUSSION

There is a close similarity in structure between the  $V_L$  domains of HyHEL-10 and REI, even in their CDRs. Also, there are similar structures for the framework parts of the  $V_H$  domain of HyHEL-10 and of the other Fabs. Further, the H-chain CDRs of HyHEL-10, D1.3, and NEW, which have the same number of residues, have similar backbone structures. This leads us to conclude that no major conformational changes have occurred in the structure of HyHEL-10 antibody upon binding to lysozyme. Minor changes may have occurred in the backbone structures of the CDR loops but these would be obscured by the relatively low resolution of the present work. Movements of side chains, most notably the ones exposed to solvent, may also have occurred. However, the determination of these changes would require a structural analysis of the uncomplexed Fab.

The differences observed at position 47 and around position 101 between the lysozyme structure in the complex with HyHEL-10 and that of lysozyme by itself may represent an adjustment of the structure of the antigen upon binding to the antibody. Alternatively, these differences may simply reflect the flexibility of lysozyme in these regions. Indeed, the crystallographic *B* factors, which are frequently used as a measure of structural mobility, for the  $\alpha$  carbons of Thr-47 and Asp-101 of lysozyme are 2.7 and 2.4 standard deviations, respectively, above the mean for all the  $\alpha$  carbons in the uncomplexed structure. Nevertheless, no major changes in the structure of the antigen are observed in this antibody-lysozyme complex.

Several factors contribute to the energy of interaction between HyHEL-10 and lysozyme. The complete exclusion of solvent molecules from the HyHEL-10-lysozyme interface contributes a large hydrophobic component to the binding energy in the form of an increase in entropy due to the release of water molecules that would normally be bound to the surface of these proteins (35, 36). Further, the involvement of many aromatic residues in this antibody-antigen interaction minimizes the loss of conformational entropy when side chains are fixed upon complex formation. Additional energy comes from the polar interactions. In this instance, charge-charge interactions contribute very little, since the only ion-pair between HyHEL-10 and lysozyme is at the edge of the interface and is exposed to solvent, so that it is probably weak.

The hydrogen-bond interactions contribute significantly to the binding energy; some of these hydrogen bonds involve charged groups and should be strong (37), and the hydrogen bonds that involve main-chain atoms should serve to anchor the two proteins more firmly to each other.

In general terms, the structure of HyHEL-10 Fab is similar to what has been found in other Fabs (1, 2, 17, 28–30). The elbow bend of 147 degrees for this liganded Fab is essentially the same as that found for the unliganded J539 Fab (28); this is further evidence that the variation in the elbow bend is not correlated with the ligand state of the antibody molecule (38) but, instead, is simply an indication of the flexibility of this part of the structure.

There are now three epitopes on lysozyme that have been located by crystallographic analyses. Of these, the HyHEL-10 epitope is the most discontinuous. Whereas the HyHEL-5 and D1.3 epitopes both consist essentially of two stretches of polypeptide chain, the HyHEL-10 epitope is most easily described as the exposed surface of a helix plus some of the surrounding structure. The central location of the helix in the HyHEL-10 epitope and the involvement of all the exposed residues in the contact suggest that the helix by itself might suffice to block the binding of HyHEL-10 to lysozyme. The epitope for NC41 Fab on the influenza virus neuraminidase is also rather discontinuous, consisting of four segments of polypeptide chain (3).

The anti-lysozyme-lysozyme complexes studied have comparable areas of interaction between antibody and antigen (about 700 Å<sup>2</sup> per molecule). Further, the binding constants are comparable (between 10<sup>7</sup> and 10<sup>10</sup> M<sup>-1</sup>). However, differences in the nature of the contacts exist. In HyHEL-5, for example, the importance of electrostatic interactions is emphasized by the presence of two salt bridges in the center of the antibody-antigen interface, involving two arginines from the antigen and two glutamic acids from the antibody (2). In the complex of HyHEL-10 with lysozyme, the one ion-pair interaction observed is weak. In the complex of D1.3 with lysozyme, no ion pairs were found (1). In all three complexes, many hydrogen bonds exist between antibody and antigen and several aromatic residues are involved in the contact. Also, in all three complexes, framework residues were found to contribute to the binding of the antigen. In D1.3 and HyHEL-10, the framework residue was immediately adjacent to a CDR; in HyHEL-5, the contacting framework residue involved was a very highly conserved tryptophan (32) that probably plays an important role in V<sub>L</sub>-V<sub>H</sub> interactions (39, 40).

The three lysozyme epitopes constitute >40% of the total surface of the lysozyme (4). This observation, together with the known existence of antibodies to other regions of lysozyme (41), strongly supports the conclusion that all accessible parts of the molecule may be antigenic (42). There is a slight overlap of the HyHEL-10 and D1.3 epitopes (around the main chain of Asn-19) that probably would preclude the simultaneous binding of these two antibodies to lysozyme. There is no overlap of the HyHEL-10 and HyHEL-5 epitopes or of the HyHEL-5 and D1.3 epitopes. Although these three epitopes are generally accessible to large probes, only parts of them encompass residues of high mobility as determined from tetragonal lysozyme (D. C. Phillips, personal communication) (4).

The epitope for HyHEL-10 includes part of the catalytic cleft of lysozyme, suggesting that binding of antibody could interfere with the enzyme's ability to bind and cleave substrate. Modeling of a hexasaccharide in the catalytic cleft of lysozyme suggests that the first two subsites are unavailable for binding in the presence of antibody. This prediction agrees well with the observation that HyHEL-10 is an efficient inhibitor of catalysis of both *Micrococcus lysodeikticus* cells and hexasaccharide (ref. 43; J. R. Rupley, personal communication). However, we have been unable to demonstrate competitive inhibition of HyHEL-10 binding to hen egg

white lysozyme utilizing oligosaccharide substrates, either at low temperature with hexa- or pentasaccharide under conditions in which both these oligosaccharides competitively inhibited binding of HyHEL-5 to lysozyme (10) or at room temperature with smaller saccharides.

- Amit, A. G., Mariuzza R. A., Phillips, S. E. V. & Poljak, R. J. (1986) *Science* **233**, 747–753.
- Sheriff, S., Silverton, E. W., Padlan, E. A., Cohen, G. H., Smith-Gill, S. J., Finzel, B. C. & Davies, D. R. (1987) *Proc. Natl. Acad. Sci. USA* **84**, 8075–8079.
- Colman, P. M., Laver, W. G., Varghese, J. N., Baker, A. T., Tulloch, P. A., Air, G. M. & Webster, R. G. (1987) *Nature (London)* **326**, 358–363.
- Davies, D. R., Sheriff, S. & Padlan, E. A. (1988) *J. Biol. Chem.* **263**, 10541–10544.
- Lavoie, T. B., Kam-Morgan, L. N. W., Mallett, C. P., Schilling, J. W., Prager, E. M., Wilson, A. C. & Smith-Gill, S. J. (1989) in *The Use of X-ray Crystallography in the Design of Antiviral Agents*, eds. Laver, G. W. & Air, G. M. (Academic, New York), in press.
- Friguet, B., Chaffotte, A. F., Djavadi-Ohanian, L. & Goldberg, M. E. (1985) *J. Immunol. Methods* **77**, 305–319.
- Harper, M., Lema, F., Boulout, G. & Poljak, R. J. (1987) *Mol. Immunol.* **24**, 97–108.
- Verhoeven, M., Milstein, C. & Winter, G. (1988) *Science* **239**, 1534–1536.
- Smith-Gill, S. J., Mainhart, C., Lavoie, T. B., Feldman, R. J., Drohan, W. & Brooks, B. R. (1987) *J. Mol. Biol.* **194**, 713–724.
- Smith-Gill, S. J., Rupley, J. A., Pincus, M. R., Carty, R. P. & Scheraga, H. A. (1984) *Biochemistry* **23**, 993–997.
- Silverton, E. W., Padlan, E. A., Davies, D. R., Smith-Gill, S. & Potter, M. (1984) *J. Mol. Biol.* **180**, 761–765.
- Xuong, N.-H., Freer, S., Hamlin, R., Nielsen, C. & Vernon, W. (1978) *Acta Crystallogr. Sect. A* **34**, 289–296.
- Rossmann, M. G., ed. (1972) *The Molecular Replacement Method* (Gordon & Breach, New York).
- Fitzgerald, P. M. D. (1988) *J. Appl. Crystallogr.* **21**, 273–278.
- Cyglar, M. & Anderson, W. F. (1988) *Acta Crystallogr. Sect. A* **44**, 38–45.
- Diamond, R. (1974) *J. Mol. Biol.* **82**, 371–391.
- Satow, Y., Cohen, G. C., Padlan, E. A. & Davies, D. R. (1986) *J. Mol. Biol.* **190**, 593–604.
- Sussman, J. L. (1985) *Methods Enzymol.* **115**, 271–303.
- Hendrickson, W. A. & Konnert, J. H. (1980) in *Computing in Crystallography*, eds. Diamond, R., Ramaseshan, S. & Venkatesan, K. (Ind. Acad. Sci., Bangalore, India), pp. 13.01–13.23.
- Cohen, G. H. (1986) *J. Appl. Crystallogr.* **19**, 486–488.
- Bhat, T. N. (1988) *J. Appl. Crystallogr.* **21**, 279–281.
- Jones, A. T. (1978) *J. Appl. Crystallogr.* **11**, 614–617.
- Bernstein, F. C., Koetzle, T. F., Williams, G. J. B., Meyer, E. F., Jr., Brice, M. D., Rodgers, J. R., Kennard, O., Shimanouchi, T. & Tasumi, M. (1977) *J. Mol. Biol.* **112**, 535–542.
- Luzzati, V. (1952) *Acta Crystallogr.* **5**, 802–810.
- Connolly, M. L. (1983) *J. Appl. Crystallogr.* **16**, 548–558.
- Case, D. A. & Karplus, M. (1979) *J. Mol. Biol.* **132**, 343–368.
- Sheriff, S., Hendrickson, W. A. & Smith, J. L. (1987) *J. Mol. Biol.* **197**, 273–296.
- Suh, S. W., Bhat, T. N., Navia, M. A., Cohen, G. H., Rao, D. N., Rudikoff, S. & Davies, D. R. (1986) *Proteins Struct. Funct. Genet.* **1**, 74–80.
- Marquart, M., Deisenhofer, J., Huber, R. & Palm, W. (1980) *J. Mol. Biol.* **141**, 369–391.
- Saul, F., Amzel, L. M. & Poljak, R. J. (1978) *J. Biol. Chem.* **253**, 585–597.
- Epp, O., Lattman, E. E., Schiffer, M., Huber, R. & Palm, W. (1975) *Biochemistry* **14**, 4943–4952.
- Kabat, E. A., Wu, T. T., Reid-Miller, M., Perry, H. M. & Gottesman, K. S. (1987) *Sequences of Proteins of Immunological Interest* (Natl. Inst. Health, Bethesda, MD), 4th Ed.
- Bjorkman, P. I., Saper, M. A., Samroui, B., Bennett, W. S., Strominger, J. L. & Wiley, D. C. (1987) *Nature (London)* **329**, 506–512.
- Phillips, D. C. (1966) *Sci. Am.* **215**, 78–90.
- Kauzmann, W. (1959) *Adv. Protein Chem.* **14**, 1–63.
- Chothia, C. (1974) *Nature (London)* **248**, 338–339.
- Fersht, A. R., Shi, J.-P., Knill-Jones, J., Lowe, D. M., Wilkinson, A. J., Blow, D. M., Brick, P., Carter, P., Wayne, M. M. Y. & Winter, G. (1985) *Nature (London)* **314**, 235–238.
- Huber, R. (1976) *Trends Biochem. Sci.* **1**, 174–178.
- Segal, D. M., Padlan, E. A., Cohen, G. H., Rudikoff, S., Potter, M. & Davies, D. R. (1974) *Proc. Natl. Acad. Sci. USA* **71**, 3298–3302.
- Poljak, R. J., Amzel, L. M., Chen, B. L., Phizackerley, R. P. & Saul, F. (1975) *Immunogenetics* **2**, 393–394.
- Arnon, R. (1977) in *Immunochemistry of Enzymes and Their Antibodies*, ed. Salton, M. R. J. (Wiley, New York), pp. 1–28.
- Benjamin, D. C., Berzofsky, J. A., East, I. J., Gurd, F. R. N., Hannum, C., Leach, S. J., Margoliash, E., Michael, J. G., Miller, A., Prager, E. M., Reichlin, M., Sercarz, E. E., Smith-Gill, S. J., Todd, P. E. & Wilson, A. C. (1984) *Annu. Rev. Immunol.* **2**, 67–101.
- Smith-Gill, S. J., Lavoie, T. B. & Mainhart, C. R. (1984) *J. Immunol.* **133**, 384–393.